CT Texture Analysis: Definitions, Applications, Biologic Correlates, and Challenges[1]

Meghan G. Lubner, MD
Andrew D. Smith, MD, PhD
Kumar Sandrasegaran, MD
Dushyant V. Sahani, MD
Perry J. Pickhardt, MD

Abbreviations: AUC = area under the receiver operating characteristic curve, CTTA = CT texture analysis, MPP = mean of the positive pixels, RCC = renal cell carcinoma, SUV = standardized uptake value, 3D = three-dimensional, 2D = two-dimensional

RadioGraphics 2017; 37:1483–1503

https://doi.org/10.1148/rg.2017170056

Content Codes: BQ CT GI GU IN OI

[1]From the Department of Radiology, University of Wisconsin School of Medicine and Public Health, E3/311 Clinical Sciences Center, 600 Highland Ave, Madison, WI 35792 (M.G.L., P.J.P.); Department of Radiology, University of Mississippi Medical Center, Jackson, Miss (A.D.S.); Department of Radiology, Indiana University School of Medicine, Indianapolis, Ind (K.S.); and Department of Radiology, Harvard Medical School, Boston, Mass (D.V.S.). Presented as an education exhibit at the 2016 RSNA Annual Meeting. Received March 13, 2017; revision requested May 8 and received June 7; accepted June 16. For this journal-based SA-CME activity, the authors M.G.L., A.D.S., K.S., and P.J.P. have provided disclosures (see end of article); all other authors, the editor, and the reviewers have disclosed no relevant relationships. **Address correspondence to** M.G.L. (e-mail: *mlubner@uwhealth.org*).

See discussion on this article by Chu (pp 1503–1505).

SA-CME LEARNING OBJECTIVES

After completing this journal-based SA-CME activity, participants will be able to:

- Describe and define different first- and second-order CT texture parameters.
- List potential applications of CTTA in differentiating benign and malignant lesions.
- Identify tumor and therapy types in which CTTA may be useful in pretreatment assessment or evaluating response to therapy.

See www.rsna.org/education/search/RG.

This review discusses potential oncologic and nononcologic applications of CT texture analysis (CTTA), an emerging area of "radiomics" that extracts, analyzes, and interprets quantitative imaging features. CTTA allows objective assessment of lesion and organ heterogeneity beyond what is possible with subjective visual interpretation and may reflect information about the tissue microenvironment. CTTA has shown promise in lesion characterization, such as differentiating benign from malignant or more biologically aggressive lesions. Pretreatment CT texture features are associated with histopathologic correlates such as tumor grade, tumor cellular processes such as hypoxia or angiogenesis, and genetic features such as KRAS or epidermal growth factor receptor (EGFR) mutation status. In addition, and likely as a result, these CT texture features have been linked to prognosis and clinical outcomes in some tumor types. CTTA has also been used to assess response to therapy, with decreases in tumor heterogeneity generally associated with pathologic response and improved outcomes. A variety of nononcologic applications of CTTA are emerging, particularly quantifying fibrosis in the liver and lung. Although CTTA seems to be a promising imaging biomarker, there is marked variability in methods, parameters reported, and strength of associations with biologic correlates. Before CTTA can be considered for widespread clinical implementation, standardization of tumor segmentation and measurement techniques, image filtration and postprocessing techniques, and methods for mathematically handling multiple tumors and time points is needed, in addition to identification of key texture parameters among hundreds of potential candidates, continued investigation and external validation of histopathologic correlates, and structured reporting of findings.

Introduction

There has been growing interest in quantitative imaging biomarkers in recent years, particularly in the evaluation of tumors and cancer response to therapy. However, as our knowledge of the molecular signatures of different tumor types improves and therapies become increasingly varied and individualized, characterization of tumor and assessment of response to therapy become increasingly complex and in many cases need to be tailored to the specific tumor and therapy type. As a result, a profusion of imaging biomarkers have emerged using advanced imaging techniques, many of which are still being validated.

TEACHING POINTS

- Texture analysis provides an objective, quantitative assessment of tumor heterogeneity by analyzing the distribution and relationship of pixel or voxel gray levels in the image.
- In a statistical-based model, first-order statistics evaluate the gray-level frequency distribution from the pixel intensity histogram in a given area of interest, including mean intensity, threshold (percentage of pixels within a specified range), entropy (irregularity), standard deviation, skewness (asymmetry), and kurtosis (peakedness/flatness of pixel histogram).
- For a variety of tumors, there are quantifiable texture differences between benign and malignant lesions (generally with greater heterogeneity in malignant lesions), possibly allowing pathologic differentiation in certain clinical scenarios.
- CTTA features are associated with histopathologic features and clinical outcomes in a variety of primary and metastatic tumors. In general, a change in tumor heterogeneity (either increased or decreased) may be associated with treatment response and improved prognosis/outcome.
- A variety of challenges, including standardization of segmentation/measurement, postprocessing (eg, use of image filtration methods), and reporting as well as ongoing delineation of pathologic correlates, need to be resolved before widespread implementation.

Figure 1. Gross specimen of a large renal cell carcinoma (RCC) demonstrates heterogeneity, which is visible to the naked eye but difficult to quantify objectively.

Tumors are heterogeneous on the gross and cellular levels, as well as the genetic and phenotypic levels, with spatial heterogeneity in cellular density, angiogenesis, and necrosis (Fig 1) (1). This heterogeneity may affect prognosis and treatment, as more heterogeneous tumors may be associated with more biologically aggressive behavior and increased resistance to treatment.

Tumor heterogeneity can be difficult to capture and quantify with traditional imaging tools, subjective assessment of images, or random sampling biopsy, which evaluates only a small part of the tumor (1). Therefore, although it is not a new tool (2), there is renewed interest in computed tomographic (CT) texture analysis (CTTA), a potentially useful biomarker that allows assessment and quantification of tumor spatial heterogeneity. CTTA is just one part of the growing field of radiomics, which comprises high-throughput extraction, analysis, and interpretation of quantitative features from medical images (3).

CTTA has shown promise in a variety of tumor types, including colorectal cancer, head and neck cancer, esophageal cancer, lung cancer, and renal cell carcinoma (RCC), in predicting pathologic features, response to therapy, and prognosis (4–8). In addition, data are emerging to show that CTTA may have utility in a variety of nononcologic applications, including assessment and quantification of hepatic fibrosis, pulmonary fibrosis, interstitial pneumonia, and emphysema (9–13). However, there are a variety of unknowns, challenges, and limitations related to CTTA that require further investigation before this potentially valuable tool is ready for mainstream application.

The purpose of this article is to review the basic concepts of texture analysis, describe oncologic and potential nononcologic applications of CTTA, evaluate histopathologic correlation with individual CTTA parameters, and discuss unknowns, limitations, and challenges around CTTA.

Basic Concepts of Texture Analysis

Texture analysis provides an objective, quantitative assessment of tumor heterogeneity by analyzing the distribution and relationship of pixel or voxel gray levels in the image (14). Different methods of texture analysis have been applied, including statistical-, model-, and transform-based methods. Statistical-based techniques have been most commonly applied, either through commercially available or in-house software tools, to describe the relationship of gray-level values in the image.

In a statistical-based model, first-order statistics evaluate the gray-level frequency distribution from the pixel intensity histogram in a given area of interest, including mean intensity, threshold (percentage of pixels within a specified range), entropy (irregularity), standard deviation, skewness (asymmetry), and kurtosis (peakedness/flatness of pixel histogram) (Fig 2). First-order histogram analysis does not account for the location of the pixels and lacks any reference to the spatial interrelationship between gray values.

Second-order statistics can be based on a co-occurrence matrix and include things like second-order entropy, energy, homogeneity, dissimilarity, and correlation. Second-order statistics can also be derived using a run-length matrix, which

Figure 2. First-order statistical-based CT texture parameters. **(a)** Plot of the pixel histogram, where the x-axis represents gray-level values or attenuation and the y-axis represents the frequency of occurrence. First-order parameters include mean or mean gray-level intensity of the histogram (vertical red line), standard deviation of the histogram (horizontal blue line), and mean of the positive pixels (MPP) (average gray-level intensity above threshold of zero) (yellow box). **(b)** Sample histograms show skewness, which is negative when skewed values are less than zero (left) and positive when skewed values are greater than zero (right). **(c)** Sample histograms show kurtosis, which describes the peakedness or pointiness of the pixel histogram. A pointier or more peaked histogram is seen with positive and progressively higher kurtosis values (right).

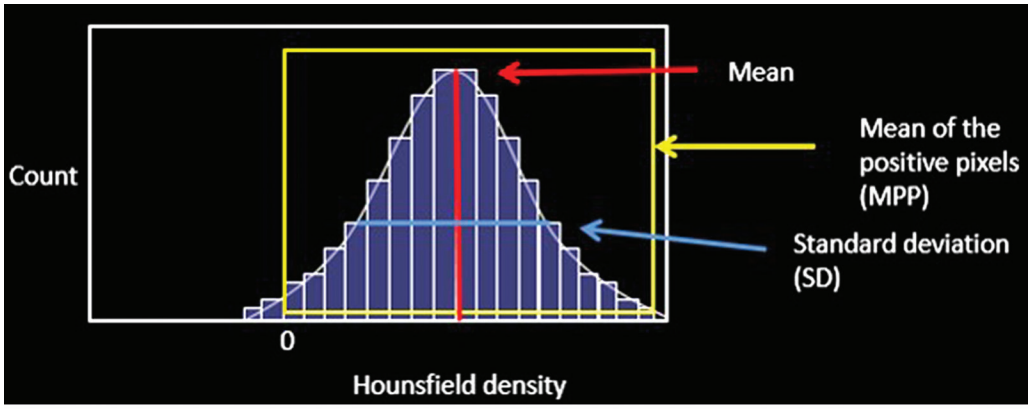

a.

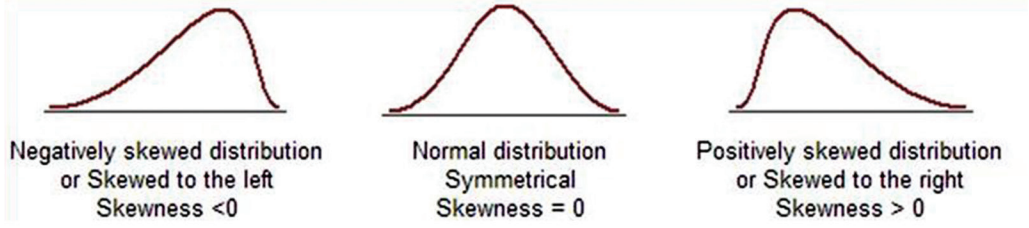

b.

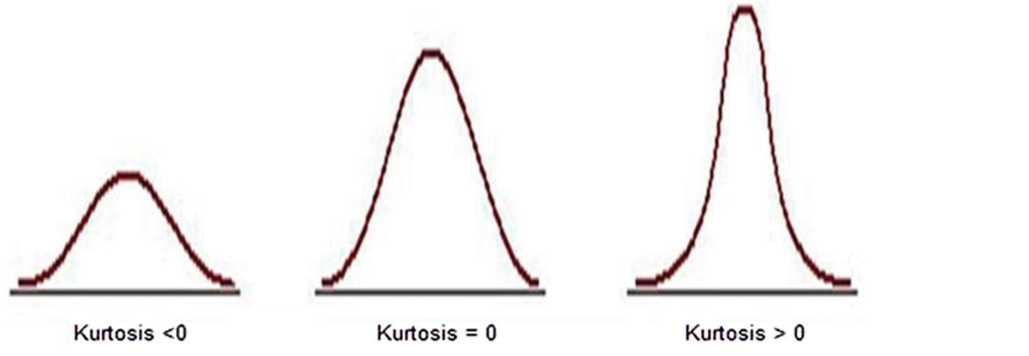

c.

analyzes texture in a specific direction. Higher-order statistics, such as contrast, coarseness, and busyness, can be calculated using neighborhood gray-tone difference matrices, which examine location and relationships between three or more pixels (Table 1). Higher-order features have the advantage of evaluating voxels in their local context, taking the relationship with neighboring voxels into account (Fig 3) (3).

To perform CTTA, postprocessing software is needed, which can be either a commercially available tool or an in-house design, most of which are CT vendor neutral. This can be performed retrospectively on images obtained in the same phase of contrast enhancement with similar technique; in general, no prospective acquisition is needed. CTTA can be performed on either single-section (eg, largest cross-sectional area) or volumetric datasets to assess tumor heterogeneity (15).

An optional image filtration step can be performed. There are a wide variety of imaging filtration methods. A Laplacian or Gaussian bandpass filter is a commonly used advanced image filtration method that alters the image pixel intensity patterns and allows extraction of specific structures corresponding to the width of the filter. Lower filter values correspond to fine

Table 1: Spectrum of Statistical-based First-Order and Higher-Order Texture Features

Texture Feature	Level/Order	Description	Examples	Comments
Intensity of pixel histogram	First order	Histogram where x-axis represents pixel/voxel gray level and y-axis represents frequency of occurrence (Fig 2)	Mean gray-level intensity, threshold, standard deviation or variance of the pixel histogram, skewness, kurtosis, first-order entropy, mean of the positive pixels (MPP)	Takes into account only pixel intensity, not spatial location or relationship of pixels First-order entropy is the irregularity or complexity of pixel intensities
Run-length matrix	Second order	Adjacent or consecutive pixels/voxels of a single gray level in a given direction	Run-length nonuniformity, gray-level nonuniformity, long-run emphasis, short-run emphasis, fraction	Similar to co-occurrence matrix, takes into account both pixel intensity and spatial relationships
Gray-level co-occurrence matrix	Second order	How often pairs of pixels with specific values in a specified spatial range occur in an image	Contrast, uniformity, second-order entropy, sum of variance, sum of averages, sum of entropy	…
Advanced metrics	Higher order	Comparing differences and relationships between multiple pixels/voxels	Hundreds: autoregressive model, Haar wavelet (wavelet energy), geometry parameters, neighborhood gray-tone difference matrix	…

Source.—Reference 3.

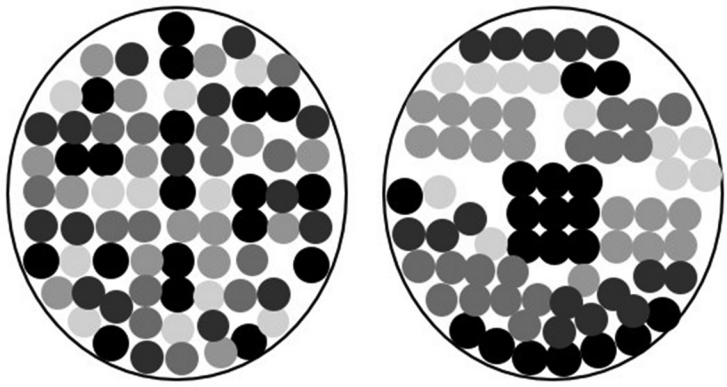

Figure 3. Diagrams of two different gray-scale images. Each of the circles contains the same number of light gray, medium gray, dark gray, and black "pixels," so the first-order texture features and pixel histograms are nearly identical for these two images. However, higher-order texture features that take into account pixel location and relationship to adjacent pixels, such as gray-level co-occurrence matrix or run-length matrix, would be different between these two images. For example, a light gray pixel occurs horizontally adjacent to and to the left of a black pixel four times in the left circle but only twice in the right circle. The gray-level co-occurrence matrix measures the frequency with which each type of pixel occurs in the horizontal, vertical, and oblique planes adjacent to all other pixels. This frequency is then mapped, representing the spatial relationship between the pixels, not just the pixels present.

texture features, while higher filter values emphasize medium or coarse texture features (Fig 4) (1). In addition, this filtration step is designed to remove noise and enhance edges, which may make measurements less susceptible to small differences in technique. Denoising or gray-level standardization steps have been used as well as a premeasurement step to help eliminate differences that are technical rather than biologic and to aid in reproducibility.

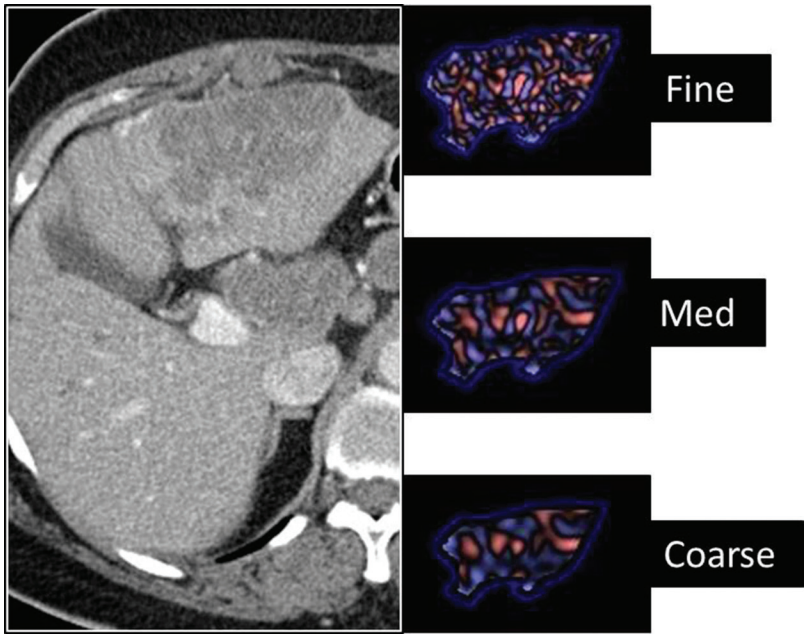

Figure 4. Single-section statistical-based CTTA of a hepatic metastatic colorectal lesion. A Laplacian of Gaussian filtration step was used, which highlights features of different sizes from fine (top right) to coarse (bottom right). The color overlay represents general attenuation of the pixels: pink or red = positive pixels, blue or purple = negative pixels. *Med* = medium.

Model-based texture analysis uses advanced mathematical methods such as fractal analysis, while transform-based methods convert spatial information into frequency and/or scale (wavelet) information (1).

At CT, there has been some concern that heterogeneity related to technique (photon noise) may mask underlying true biologic heterogeneity, but studies have demonstrated that texture analysis at CT is feasible by reducing the effect of photon noise (16–18) using image filtration. Other studies have shown that some but not all texture features applied to unfiltered or filtered images have high interobserver agreement (19).

Oncologic Applications

Potential oncologic applications of CTTA remain an active area of research. These applications seem to fall into three main categories: lesion characterization, pretreatment assessment (of both primary tumors and metastatic disease), and initial posttreatment assessment in reference to baseline tumor heterogeneity to predict therapeutic response.

Lesion Characterization

A major diagnostic challenge is to accurately differentiate benign from malignant lesions using noninvasive methods. For a variety of tumors, there are quantifiable texture differences between benign and malignant lesions (generally with greater heterogeneity in malignant lesions), possibly allowing pathologic differentiation in certain clinical scenarios. CTTA has the potential to function as a "virtual biopsy" of indeterminate masses.

Kidney.—Differentiating benign from malignant renal lesions is a challenging imaging task. Raman et al (20) used CTTA to differentiate renal cysts, oncocytomas, clear cell RCC, and papillary RCC (n = 20 each; Fig 5). They found that clustered CTTA features (mean, standard deviation, entropy) in a random forest model allowed correct categorization of cysts in 100% of cases, oncocytoma in 89%, clear cell RCC in 91%, and papillary RCC in 100%.

Several groups have evaluated the utility of CTTA in differentiating lipid-poor angiomyolipomas (AMLs) from RCC. Yan et al (21) found good-to-excellent classification of fat-poor AML versus papillary RCC and clear cell RCC. Hogdon et al (22) found lower lesion homogeneity and higher entropy in RCC than in lipid-poor AMLs at nonenhanced CT. The group of texture features showed an area under the receiver operating characteristic curve (AUC) of 0.89 in differentiating these lesions and performed better than subjective assessment. Another group found that skewness, among other CT features, may help identify fat in AMLs that is not visible on conventional images (23).

Leng et al (24) studied 158 resected small renal masses (<4 cm), which consisted of clear cell RCC (n = 98), papillary RCC (n = 36), and lipid-poor AMLs (n = 24). Clear cell RCC was more heterogeneous (both subjectively and objectively using texture features including standard deviation, entropy, and uniformity) than papillary RCC or lipid-poor AMLs. However, subjective assessment of heterogeneity performed better than CTTA features in differentiating clear cell RCC from papillary RCC,

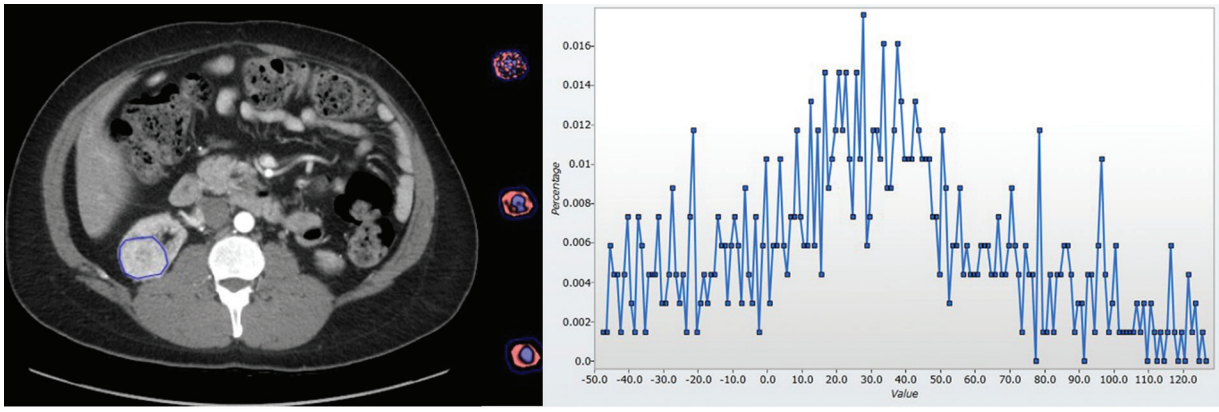

a.

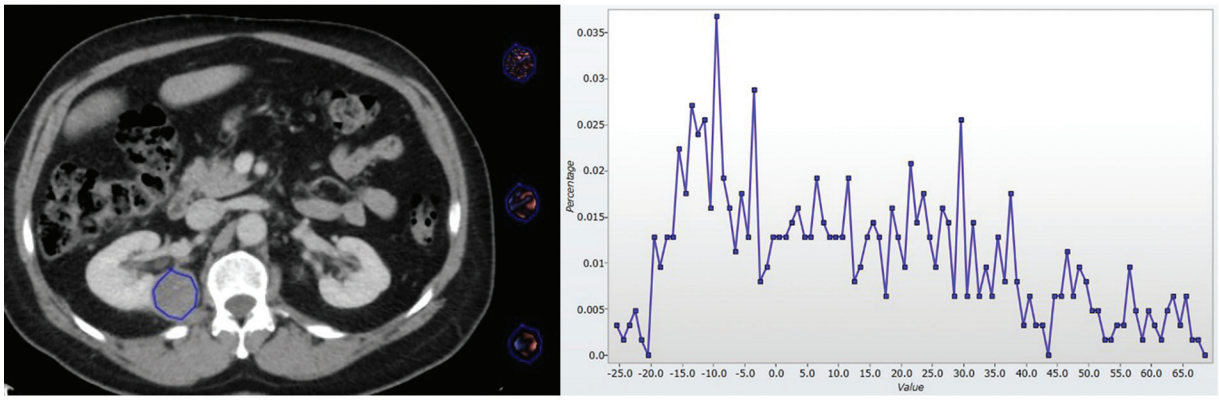

b.

Figure 5. Renal lesions with differences in heterogeneity that can be quantified and used to differentiate lesion types. **(a)** Left: CT image shows a medium clear cell RCC (blue outline). Middle: Filtered images with color overlay obtained with fine (top), medium (middle), and coarse (bottom) filters. Right: Pixel histogram. With the coarse filter, the lesion shows entropy of 4.9, mean gray-level intensity of 30.4, standard deviation of 39.2, and MPP of 45.77. **(b)** CTTA of a papillary RCC (blue outline) with associated filtered images and pixel histogram. The lesion shows entropy of 4.32, mean gray-level intensity of 12.4, standard deviation of 22.55, and MPP of 25.7. It is visually and texturally different from that in **a**: less heterogeneous and generally low in attenuation. *(Continues)*

with an AUC of 0.91 for subjective assessment versus 0.81 for standard deviation, the best-performing texture parameter. Differentiation of papillary RCC from lipid-poor AMLs proved more challenging, as both tumors were subjectively and objectively homogeneous. The authors also applied a denoising algorithm in an attempt to improve assessment of biologic heterogeneity, but results were only slightly improved.

Liver.—Another important imaging task is differentiating benign from malignant portal vein thrombus. Canellas et al (25) studied 117 patients with portal vein thrombus. They found that texture features including MPP and entropy had AUCs of 0.97 and 0.93, respectively, and 0.99 when combined, in differentiating bland (benign) thrombus from malignant (tumor) thrombus. Texture features performed better than mean Hounsfield unit attenuation alone (AUC = 0.91) and radiologists' subjective interpretation (AUC = 0.61) (Fig 6).

Another group looked at use of CTTA in differentiating hypervascular liver lesions including focal nodular hyperplasia, hepatic adenomas, and hepatocellular carcinoma. Using a random forest model, they were able to differentiate these lesion types. Predicted classification performance accuracy was 91.2% for adenoma, 94.4% for focal nodular hyperplasia, and 98.6% for hepatocellular carcinoma (26).

Pancreas.—Differentiating pancreatic cystic lesions that are benign from those with malignant potential using routine CT image evaluation is difficult. In a retrospective study (27), CTTA was used to differentiate pathologically proven intraductal papillary mucinous neoplasms (IPMNs) with high-grade dysplasia (n = 34) from those with low-grade dysplasia (n = 19). CTTA performed better in identifying lesions with high-grade dysplasia (higher risk for developing malignancy) than did use of imaging features based on the Fukuoka criteria.

The best texture feature had an AUC of 0.82, with sensitivity of 85% and specificity of 68% at the optimum threshold. The best logistic regression

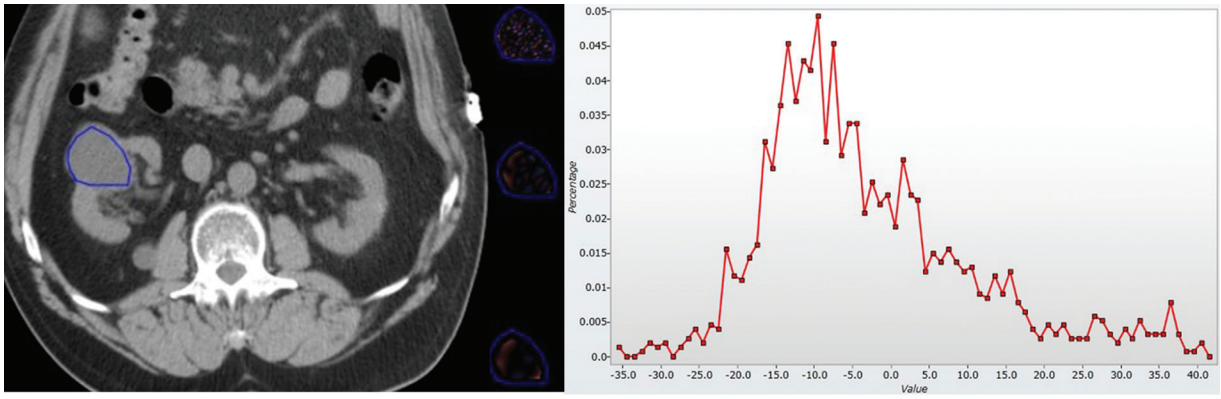

c.

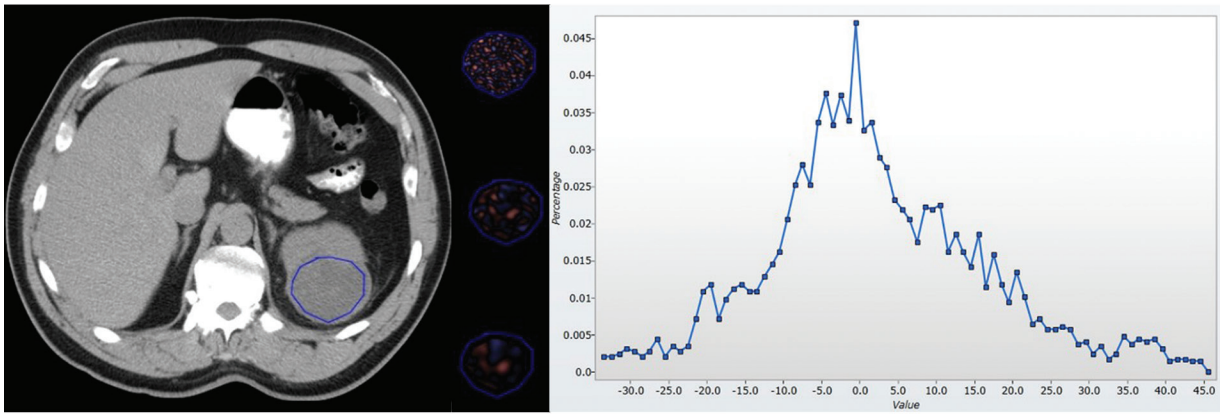

d.

Figure 5. *(Continued)* **(c, d)** CTTA of a renal cyst (blue outline in **c**) and a low-attenuation RCC (blue outline in **d**), which could be more difficult to differentiate with visual inspection alone. **(c)** The cyst shows entropy of 3.87, mean gray-level intensity of −3.15, standard deviation of 13.49, MPP of 12.34, skewness of 0.97, and kurtosis of 0.82. **(d)** The RCC is a clear cell RCC and shows entropy of 4.01, mean gray-level intensity of 2.11, standard deviation of 14.11, MPP of 12.66, skewness of 0.37, and kurtosis of 0.27. The RCC is subtly more heterogeneous, and the shape of the histogram is slightly shifted: this may aid in raising concern that this RCC is not simple and requires further evaluation.

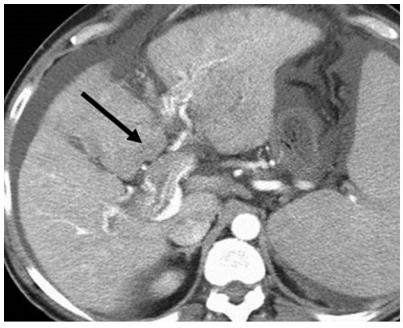

a.

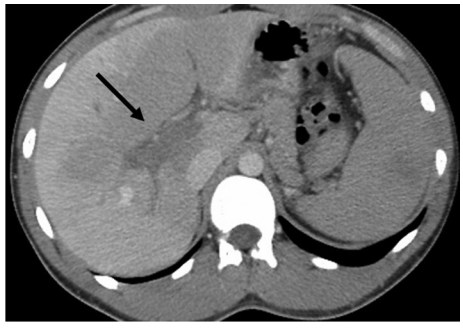

c.

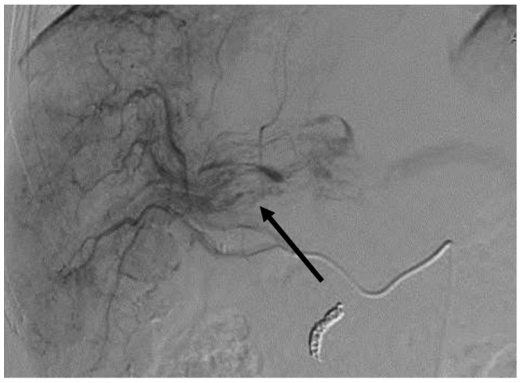

b.

Figure 6. **(a, b)** Contrast-enhanced CT image **(a)** and conventional angiogram **(b)** show tumor thrombus (arrow), which demonstrates internal threads and streaks of enhancement and is heterogeneous. **(c)** CT image shows bland thrombus (arrow), which is more homogeneous. CTTA allows quantification of heterogeneity, which can be helpful in more challenging or subtle cases.

Table 2: Lesion Characterization with CTTA

Study and Reference	Organ	Lesion Type and Number	Imaging Technique	2D versus 3D Imaging	Texture Measure	Statistical Correction or Validation	Comments
Raman et al (20)	Kidney	Renal cyst (20), oncocytoma (20), ccRCC (20), pRCC (20)	CECT (renal mass protocol): arterial, venous, delayed	Multiple sections (maximum = 10)	GLH (TexRAD, Cambridge, England)	RFM, external validation in 19 cases, OOB error calculation	RFM classification: cyst 100%, oncocytoma 89%, ccRCC 91%, pRCC 100%
Yan et al (21)	Kidney	FP AML (18), ccRCC (18), pRCC (14)	Nonenhanced CT, CECT (CMP, NP); gray-level normalization	One to four sections	GLH, RLM, GLCM, gradient, autoregressive model, wavelet (MaZda)	No	Histogram and GLCM features: excellent classification of FP AML vs ccRCC, ccRCC vs pRCC, FP AML vs pRCC; better than subjective analysis
Hogdon et al (22)	Kidney	FP AML (16), RCC (84) (51 ccRCC, 20 chRCC, 13 pRCC pooled)	Nonenhanced CT, scanner vendor heterogeneity, image intensity normalization	Three sections	GLH, GLCM, RLM (MaZda, Technical University of Lodz, Poland)	10-fold cross-validation, Holm-Bonferroni procedure	Low homogeneity and high entropy in RCC; CTTA accuracy 83%–91%, better than subjective assessment; AUC 0.85–0.89; reproducibility of contour (inter-, intra-); reproducibility of measures (CT1 vs CT2)
Takahashi et al (23)	Kidney	AML (38), RCC (83)	Nonenhanced CT	Two sections (single-section small lesions)	GLH (Matlab, MathWorks, Natick, Mass)	No	Six or more pixels < −30 HU and skewness < −0.4 in 20 of 38 AMLs vs one of 83 RCCs; slightly better than subjective analysis (52% sensitivity, 99% specificity)
Leng et al (24)	Kidney	158 SRMs (<4 cm): ccRCC (98), pRCC (36), AML (24)	CECT ± denoising algorithm	Single section	GLH: SD, entropy, uniformity (Matlab)	No	ccRCC more heterogeneous (ccRCC vs pRCC AUC 0.91, 0.81, 0.78, 0.78 for subjective analysis/SD/entropy/uniformity); no difference between pRCC and AML; slight improvement in ccRCC vs pRCC AUC with weak denoising
Canellas et al (25)	Liver	117 PVTs (63 malignant, 54 bland)	CECT (portal venous)	Single section	GLH (TexRAD)	No	MPP (AUC 0.97), entropy (AUC 0.93), combined (AUC 0.99), attenuation (AUC 0.91) all better than subjective analysis (AUC 0.61)
Hanania et al (27)	Pancreas	53 IPMNs (34 HG, 19 LG)	CECT	Not reported	GLCM	Cross-validation	Best single-marker AUC 0.82 for LG vs HG, best logistic regression AUC 0.96, better than use of Fukuoka criteria
Hu et al (28)	Colon	384 CR polyps	Nonenhanced CT (CTC)	Volume	Intensity, gradient, curvature, GLCM	Training/testing dataset, OOB error calculation	RFM AUC 0.80 for differentiating neoplastic from nonneoplastic polyps
Song et al (29)	Colon	148 total: 35 nonneoplastic, 72 TAs, 36 TVAs, five adenomas	Nonenhanced CT (CTC)	Volume	Intensity, gradient, curvature, GLCM	SVM model, training and test set	AUC 0.74 for differentiating polyps on the basis of image intensity alone, improved to 0.85 when texture features added
Pooler et al (30)	Colon	63 CR masses ≥ 3 cm (32 adenocarcinomas, 31 adenomas)	Nonenhanced CT (CTC)	Volume	Intensity, gradient, curvature, GLCM	Previously established RFM method	CTTA AUC 0.936, better than human readers' AUC of 0.917

Note.—AML = angiomyolipoma, ccRCC = clear cell RCC, CECT = contrast-enhanced CT, chRCC = chromophobe RCC, CMP = corticomedullary phase, CR = colorectal, CTC = CT colonography, FP = fat-poor, GLCM = gray-level co-occurrence matrix, GLH = gray-level histogram, HG = high grade, IPMN = intraductal papillary mucinous neoplasm, LG = low grade, NP = nephrographic phase, OOB = out-of-bag, pRCC = papillary RCC, PVT = portal vein thrombus, RFM = random forest model, RLM = run-length matrix, SD = standard deviation, SRM = small renal mass, SVM = support vector machine, TA = tubular adenoma, TVA = tubulovillous adenoma, 3D = three-dimensional, 2D = two-dimensional.

Figure 7. **(a, b)** Contrast-enhanced axial **(a)** and coronal **(b)** CT images show a large pancreatic cystic lesion with thick septa and nodular enhancement, which is clearly heterogeneous. **(c, d)** Corresponding axial **(c)** and coronal **(d)** CT images show a small simple cystic lesion. The heterogeneous lesion contains a component of invasive cancer, while the more homogeneous lesion has been stable for years. Quantitative texture analysis may be helpful in identifying more aggressive cystic lesions under surveillance and expediting intervention when necessary.

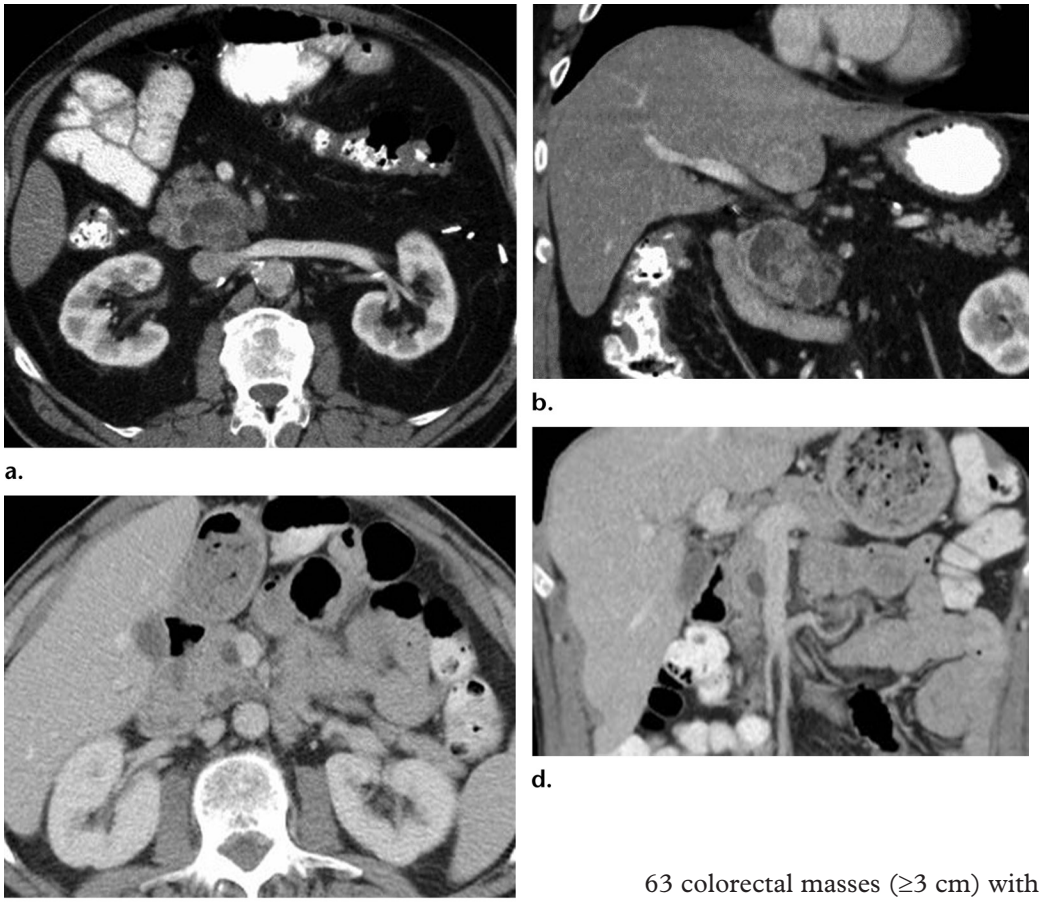

model had an AUC of 0.96, sensitivity of 97%, and specificity of 88%. Use of the Fukuoka criteria had a false-positive rate of 36% (Fig 7).

Bowel.—Multiple studies have evaluated the utility of CTTA in assessing colorectal polyps, which can have a variety of underlying histopathologic features, as well as a spectrum of biologic behavior. Traditionally, colonic polyps have been assessed using size and morphologic features (eg, flat versus nonflat). In a study of 384 polyps, CT texture features had an AUC of 0.80 for differentiating neoplastic from nonneoplastic polyps (28).

In another study, the same group evaluated 148 colonic lesions, 35 of which were nonneoplastic (29). They found an AUC of 0.74 for classifying neoplastic versus nonneoplastic lesions or hyperplastic versus adenomatous polyps when using image intensity alone, compared with an AUC of 0.85 when texture features like gradient and curvature were included. In an assessment of 63 colorectal masses (≥3 cm) with 32 adenocarcinomas and 31 advanced adenomas, Pooler et al (30) reported an AUC of 0.94 for using texture features to differentiate cancers from advanced adenoma (Fig 8).

Chest.—CTTA has also been applied to differentiating benign from malignant entities in the chest. It has been used to differentiate benign from malignant pulmonary nodules and mediastinal lymph nodes (3,31–34) and to differentiate radiation fibrosis from recurrent lung cancer (3,35,36).

A summary of studies on lesion characterization with CTTA is presented in Table 2.

Primary Tumor Assessment

There is a growing body of literature evaluating the biology of tumors before treatment. CTTA features are associated with histopathologic features and clinical outcomes in a variety of primary and metastatic tumors. In general, a change in tumor heterogeneity (either increased or decreased) may be associated with treatment response and improved prognosis/outcome. These data suggest that texture features may be useful in treatment planning and prognostication.

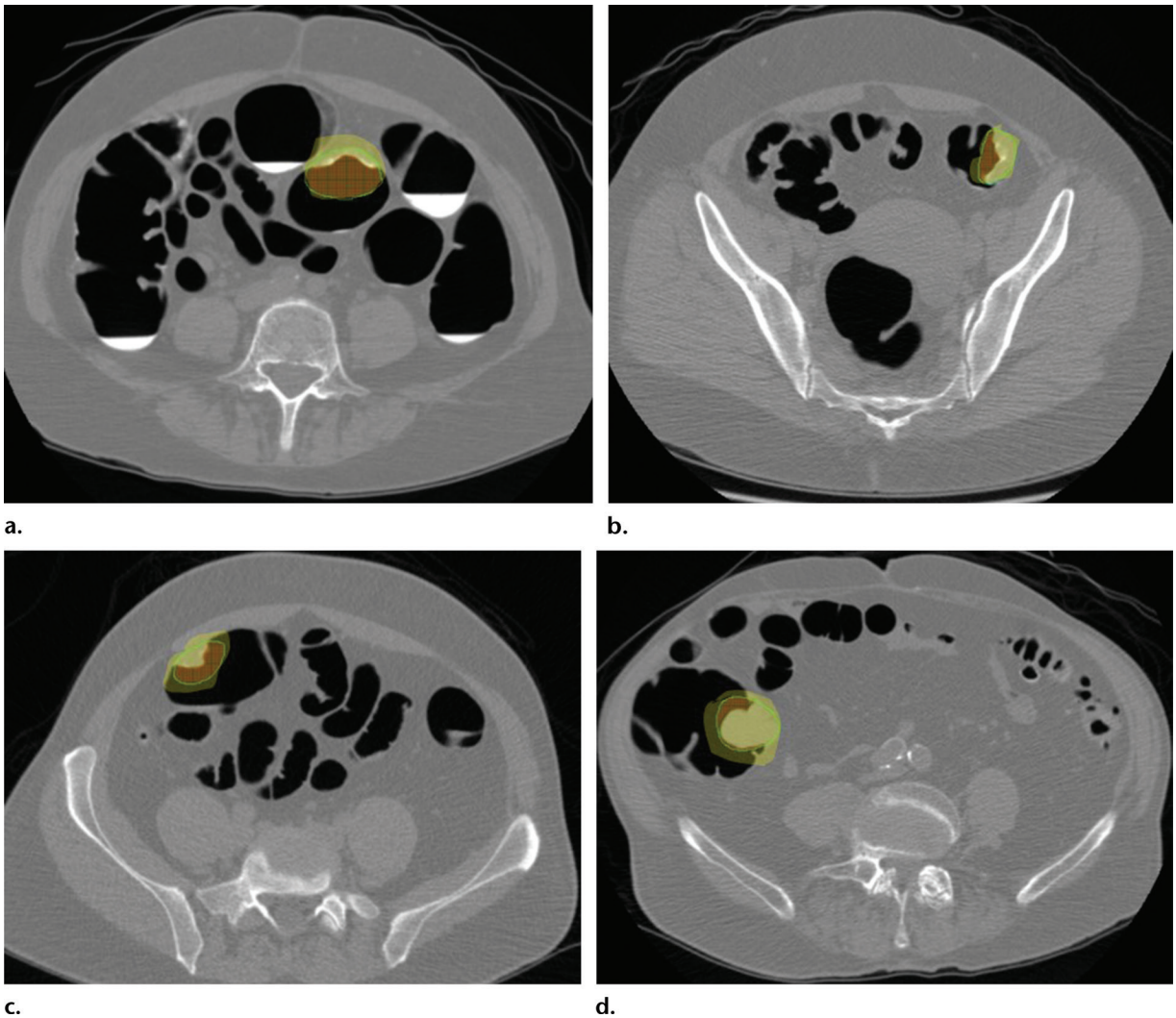

Figure 8. Texture analysis for distinguishing benign from malignant colorectal masses. Images from CT colonography show colorectal masses (highlighted in color) that were segmented semiautomatically for volumetric texture analysis. **(a, b)** Sigmoid masses: benign tubulovillous adenoma with high-grade dysplasia **(a)** and invasive adenocarcinoma **(b)**. **(c, d)** Cecal masses: benign tubulovillous adenoma with high-grade dysplasia **(c)** and invasive adenocarcinoma **(d)**. At subjective evaluation, at least one of the three readers misclassified a mass as benign or malignant in three of these four cases (all but **b**).

Genitourinary Malignancies.—One study evaluated 157 patients with a large RCC (>7 cm) and found that texture features including entropy, standard deviation, and MPP were associated with histologic subtype (clear cell, papillary, chromophobe) and nuclear grade (37) (Fig 9). Those same texture features were associated with time to recurrence and overall survival. In another study, kurtosis was associated with neovascularity (CD135/CD31) and Ki-67 in small renal masses (38).

Schieda et al (39) evaluated whether CT findings, including CTTA features, could allow differentiation of sarcomatoid RCC (n = 20) from clear cell RCC (n = 25), a distinction that would dramatically change treatment and prognosis and can be challenging to consistently make at routine biopsy. They found that sarcomatoid RCCs were in general larger than clear cell RCC. In assessing conventional CT images, the only significant features in differentiating sarcomatoid RCC were peritumoral neovascularity (higher in sarcomatoid RCC, P = .001) and size of peritumoral vessels (larger in sarcomatoid RCC, P < .001). However, objective CTTA measures such as greater run-length nonuniformity (P = .03) and greater gray-level nonuniformity (P = .04) were associated with sarcomatoid RCC (suggesting that these tumors are more heterogeneous) rather than clear cell RCC (Fig 9). The combined textural features allowed identification of sarcomatoid RCC with an AUC of 0.81.

Zhang et al (40) evaluated 105 patients with urothelial carcinomas (106 high grade, 18 low grade). They found that low-grade tumors were less heterogeneous, with significantly lower mean gray-level intensity, entropy, and MPP than high-grade tumors. MPP less than 24.1 on nonenhanced images was the optimal texture parameter for differentiating high-grade from low-grade

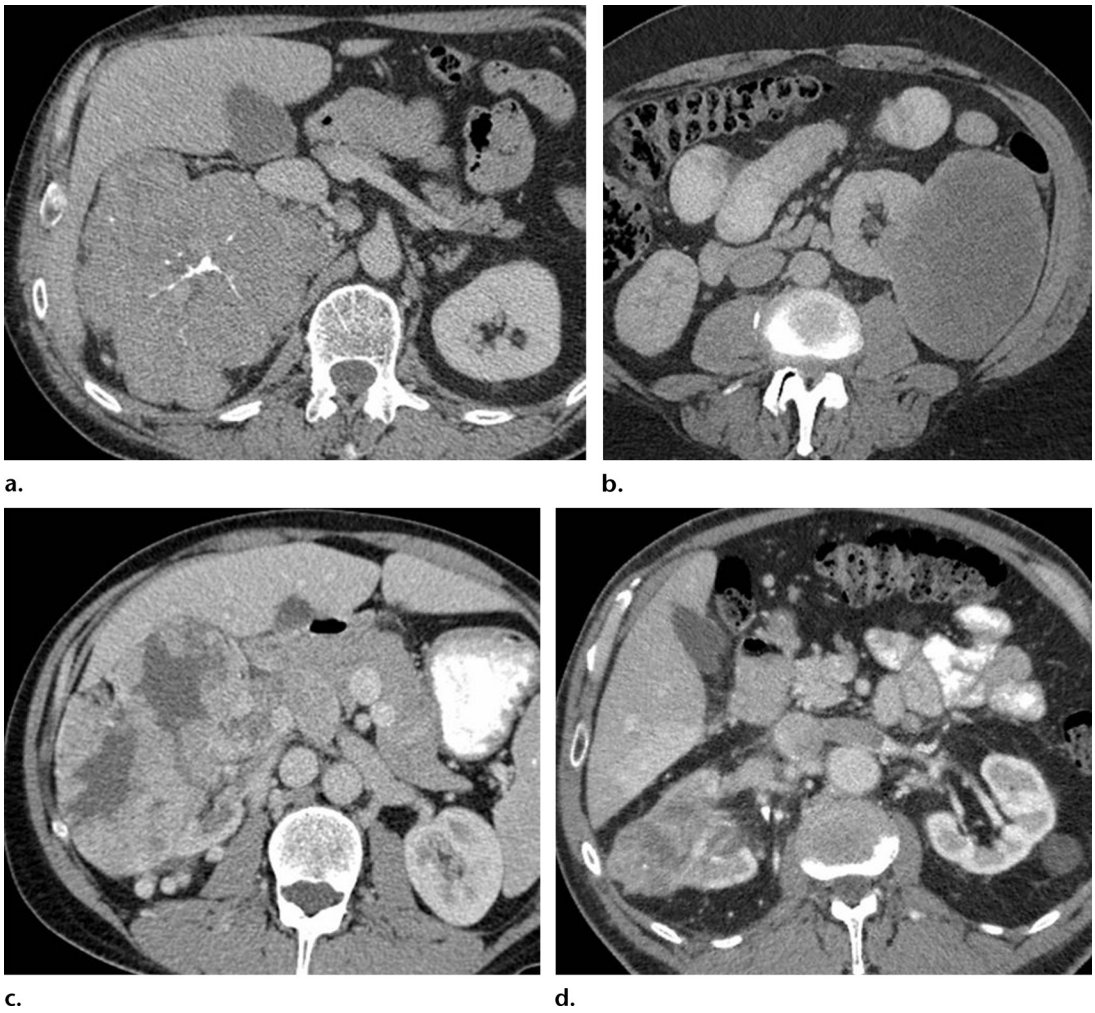

Figure 9. CT images show different types of large RCCs: chromophobe RCC **(a)**, papillary RCC **(b)**, clear cell RCC **(c)**, and clear cell RCC with 50% sarcomatoid features **(d)**. As with the spectrum of renal lesions shown in Figure 5, these known renal carcinomas increase in heterogeneity as they increase in aggressiveness.

tumors, with AUC of 0.78, sensitivity of 72%, and specificity of 85%.

Hepatopancreaticobiliary Malignancies.—Sandrasegaran et al (41) used CTTA to assess 60 patients with nonmetastatic pancreatic ductal adenocarcinoma before treatment. They found that low kurtosis correlated with poor overall survival and that higher MPP (threshold of >29.4) was associated with better progression-free survival (Fig 10). However, they also found that subjective observation of local vascular invasion (which makes the tumor unresectable) and the presence of metastatic disease were more strongly associated with prognosis.

A study of 59 patients with pancreatic neuroendocrine tumors (PNETs) found that CTTA parameters including mean attenuation, MPP, skewness, kurtosis, and entropy allowed distinction between low-grade and high-grade PNETs (AUC ranging from 0.75 to 0.85 for different levels of filtration, all $P < .001$) (42).

Hepatocellular Carcinoma.—CTTA has been found to be useful in imaging assessment of hepatocellular carcinoma (HCC). One study evaluated 130 large HCCs (>5 cm) treated with liver resection ($n = 86$) or transarterial chemoembolization (TACE) ($n = 44$) and found that texture features could be used to predict overall survival and may be useful in making treatment decisions (surgery vs embolization) (43). Another group investigated 261 HCCs treated with TACE ($n = 197$) or TACE plus sorafenib ($n = 64$) and found that a similar texture feature (wavelet 3D) was associated with overall survival and time to progression (44). In addition, texture features could be used to determine treatment regimen, with patients with lower wavelet 3D showing improved outcomes with TACE plus sorafenib.

Other Gastrointestinal Malignancies.—Studies have evaluated the value of CTTA in esophageal, gastric, and colonic cancers. Ganeshan et al (45) evaluated 21 patients with esophageal

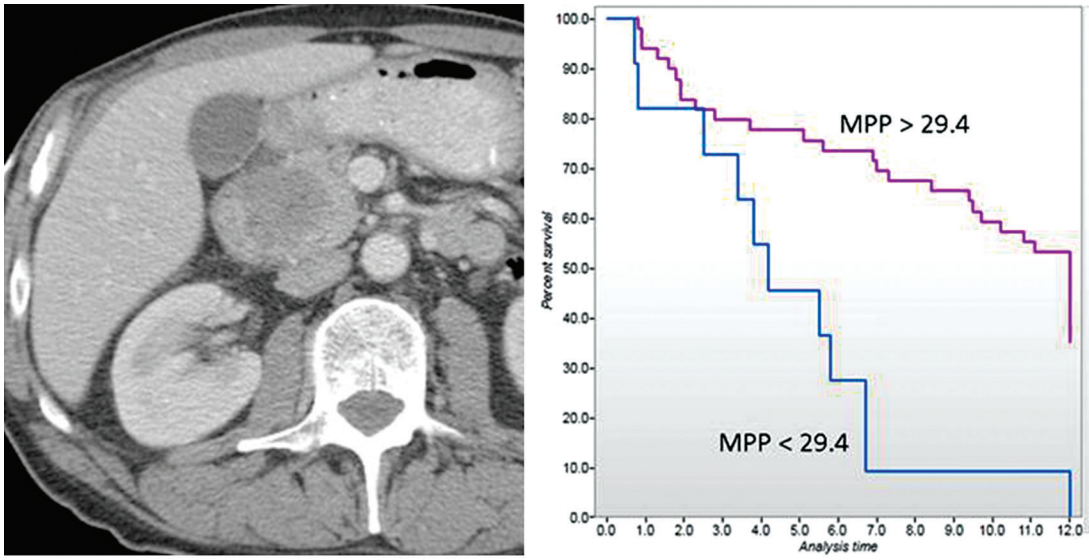

a. **b.**

Figure 10. **(a)** Axial CT image shows a pancreatic ductal adenocarcinoma without metastatic disease, which is lower in attenuation than the background parenchyma but with relatively high MPP. **(b)** Kaplan-Meier curve shows that tumors with higher MPP values have an improved prognosis (41).

cancer using nonenhanced CT images with texture analysis and positron emission tomography (PET) standardized uptake values (SUVs) and found that tumor heterogeneity correlated with fluorodeoxyglucose (FDG) uptake, SUV_{max}, and SUV_{mean}. Heterogeneity was greater in patients with clinical stage III or IV disease (entropy, uniformity) and was an independent predictor of survival. Another study evaluated 26 patients with HER2 (human epidermal growth factor receptor 2)–positive advanced gastric cancer and found that texture features including contrast, variance, and correlation allowed stratification of patients into favorable and unfavorable survival groups with an AUC greater than 0.7 (46).

Ng et al (6) evaluated primary colorectal tumors in 55 patients by using volumetric texture assessment with filtration and found that multiple texture features (entropy, uniformity, kurtosis, skewness, standard deviation) were predictive of survival and independent of tumor stage. Colorectal tumors with lower entropy, lower kurtosis, and lower standard deviation (ie, more homogeneous tumors) had a poorer prognosis, which was somewhat counterintuitive and different from results of prior studies. However, another study used CTTA in pretreatment assessment of hepatic metastatic colorectal cancer and found similar results, with entropy and standard deviation negatively associated with tumor grade (more homogeneous tumors were more likely to be higher grade) and with entropy negatively associated with survival (47) (Figs 4, 11).

CTTA has been applied to predicting development of hepatic metastatic disease by analyzing the whole liver, or nondiseased portions of the liver, before treatment or development of metastatic disease. One group found that temporal changes in hepatic texture during dynamic contrast-enhanced CT were qualitatively different from changes in enhancement and that there were differences in hepatic texture features in patients with node-negative versus node-positive colorectal cancer (16). This is an important clinical differentiation, as patients with node-positive disease are at higher risk for developing metastatic disease; node-positive patients receive adjuvant chemotherapy as a result (48). Entropy was also directly correlated with patient survival, and patients with lower entropy (less heterogeneous liver) had poorer survival (49). CTTA features were compared with the hepatic perfusion index at perfusion CT, and CTTA was a superior predictor of survival (50).

Another study looked at three cohorts of patients: those with no hepatic metastatic disease, those with synchronous hepatic metastatic disease, and those with metachronous metastatic disease within 18 months (51). The background unaffected liver was found to be significantly different at CTTA in patients with and patients without metastatic liver disease. Unlike in other studies, patients with synchronous metastatic disease had higher entropy and lower uniformity than those with no metastatic disease. There were no significant CTTA differences in the patients without metastatic disease during the follow-up period and in those who developed metachronous metastatic disease (51).

Another study used a similar cohort of patients with colorectal cancer who never developed metastatic disease compared with a cohort of patients who developed metachronous hepatic

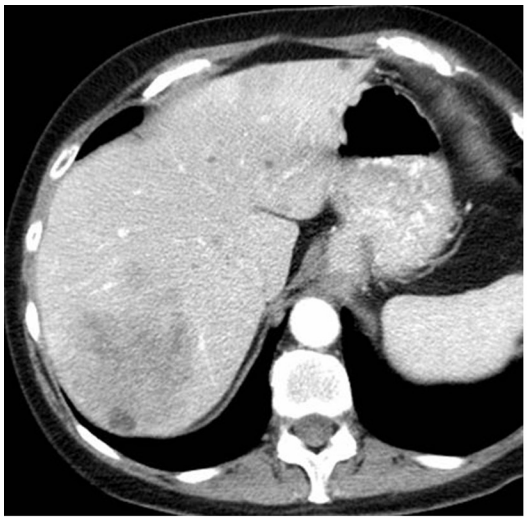

a.

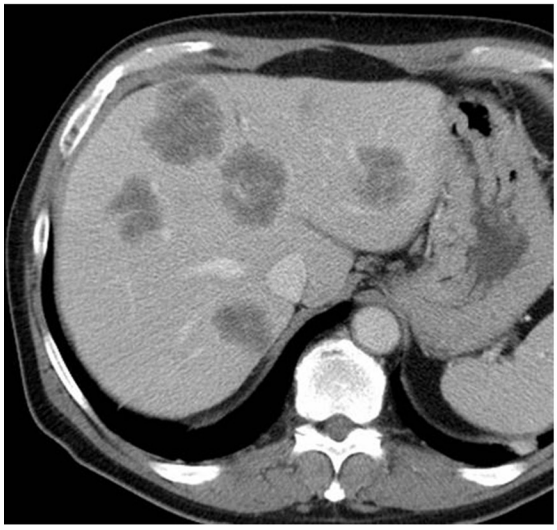

b.

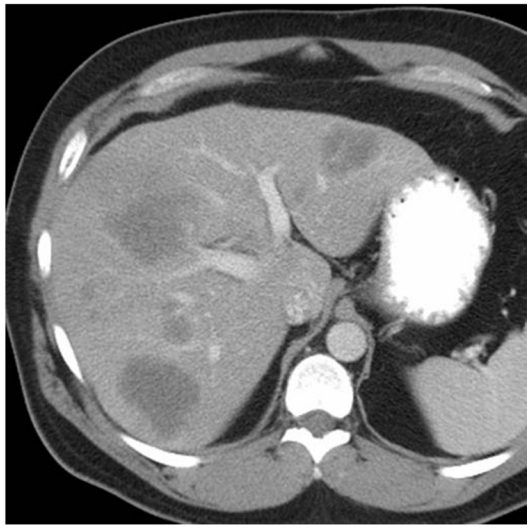

c.

Figure 11. Hepatic metastatic colorectal cancer in three patients. **(a)** Contrast-enhanced portal venous phase CT image shows a large heterogeneous lesion in the posterior right hepatic lobe that was a grade I tumor. **(b)** Corresponding image shows multiple low-attenuation but heterogeneous lesions that were grade II tumors. **(c)** Corresponding image shows hepatic lesions that appear slightly more homogeneous, but were grade III and KRAS mutant. In contradistinction to many tumors, it seems that with colorectal tumors, more homogeneous tumors are more aggressive and associated with a worse prognosis, seen with both primary and hepatic metastatic lesions (6,47).

metastatic disease (52). Results of both baseline CT and follow-up CT just before development of metastatic disease (or CT at a similar time point from baseline in the control cohort) were assessed. There were no significant differences in the previously described texture features between the two groups (no texture feature was predictive of which patients developed metastatic disease). No texture features were associated with survival. The reason for the differences in entropy that correlated with survival seen in the earlier studies is not clear; while one would have thought it was related to the development of metachronous hepatic metastatic disease, this has not been borne out in subsequent studies. This remains a somewhat controversial area of active study and warrants additional investigation given the slightly discordant results.

Multiple studies have evaluated use of CTTA features in identifying KRAS mutations in colorectal cancer. About 30%–40% of colon cancers exhibit a KRAS mutation, which is clinically significant because colorectal cancers bearing a KRAS mutation are resistant to drugs targeted against epidermal growth factor receptors (EGFRs). CTTA has shown some association with KRAS status, although limited data are available to date. In one study, the MPP was used in combination with fluorodeoxyglucose uptake and CT perfusion to identify KRAS mutants and to categorize their phenotype (hypoxic vs proliferative) (5). Other studies have shown a weak association between skewness and kurtosis and KRAS mutational status, although no statistically significant relationship was identified (47). This is an area of ongoing research.

Thoracic Malignancies.—Multiple studies have evaluated pretreatment assessment of lung cancer, particularly non–small cell lung cancer (NSCLC) (3). Some of these studies included more detailed analyses of histopathologic correlates underlying certain texture features, and several studies have

suggested that texture features may be related to the tumor microenvironment and the presence of features such as hypoxia and angiogenesis.

Ganeshan et al (53) looked at 14 resected NSCLC tumors and assessed markers for hypoxia (pimonidazole and glucose transporter 1 [GLUT-1]) and angiogenesis (CD34). They found associations with several histogram-based texture features including standard deviation, MPP, and uniformity of the positive pixels (UPP). MPP showed a significant inverse association with tumor CD34 expression (angiogenesis). Standard deviation and MPP showed a positive correlation with pimonidazole staining (hypoxia).

Weiss et al (54) found that a five-node decision tree was 90% accurate in predicting KRAS mutation status, with positive skewness and low kurtosis significantly associated with the presence of a KRAS mutation, somewhat similar to the trends described in colorectal cancer (3). Not surprisingly, they also found that kurtosis was an independent predictor of patient survival in these patients. Several other groups have shown associations between CT texture features and EGFR mutation status and other genetic features as well (55–57).

Multiple studies have demonstrated an association between CT texture features and survival in NSCLC, independent of tumor stage and other clinical factors (3). Ganeshan et al (58) found that increasing entropy and decreasing uniformity (increased tumor heterogeneity) were moderately correlated with SUV_{mean}, a prognosticator of poor outcome in lung cancer. A follow-up study demonstrated that CT texture features were also independently associated with survival in patients with NSCLC (4). Another group evaluated 98 patients with unresectable NSCLC to be treated with definitive chemotherapy–radiation therapy and found that entropy, skewness, and mean gray-level intensity were significantly associated with 3-year overall survival (higher entropy, higher or more positive skewness, and higher mean gray-level intensity were associated with poorer prognosis) (59).

In a group of 35 patients with advanced NSCLC to be treated with antiangiogenic chemotherapy, fluorodeoxyglucose uptake, CT perfusion, and CT texture features were assessed (60). High MPP, low entropy, and low SUV_{max} were associated with favorable progression-free survival. At multivariate analysis, entropy was the only independent prognostic factor for overall survival. In general, most data in NSCLC suggest that more heterogeneous tumors are more aggressive and associated with poorer prognosis/survival (3,61).

Other Tumors.—In a study of 45 patients with Hodgkin lymphoma (n = 18) and high-grade non-Hodgkin lymphoma (n = 27), CT texture features were associated with interim PET response and progression-free survival (62).

In a study of 72 patients with locally advanced squamous cell carcinoma of the head and neck, one group found that primary mass size, N stage, and primary mass entropy and skewness were independently associated with overall survival at multivariate analysis (8). In another study, 46 patients with squamous cell carcinoma of the head and neck with known human papillomavirus (HPV) status of the tumors (10 HPV positive, 36 HPV negative) were evaluated with CTTA (63). There were significant differences in 16 texture parameters (including five histogram features, three gray-level co-occurrence matrix features, one gray-level run-length feature, two gray-level gradient matrix features, and five Law features) between the HPV-positive and HPV-negative tumors. HPV-positive tumors tend to occur in younger patients and have an overall more favorable prognosis.

A summary of studies on pretreatment assessment with CTTA is presented in Table 3.

Response to Therapy

Multiple studies have investigated use of CTTA as an adjunct to conventional imaging findings, like size or CT attenuation, to determine the response of tumors to therapy. CTTA features are associated with histopathologic features and clinical outcomes in a variety of primary and metastatic tumors. In general, a change in tumor heterogeneity (either increased or decreased) may be associated with treatment response and improved prognosis/outcome.

Smith et al (19) studied 42 patients with melanoma being treated with antiangiogenic therapy who had stable disease according to the Response Evaluation Criteria in Solid Tumors (RECIST). Absolute change in MPP, change in tumor size, and baseline lactate dehydrogenase level were predictors of overall survival. A prognostic index incorporating these three factors was highly accurate for predicting overall survival at 18 months (AUC = 0.91) (Fig 12).

Goh et al (64) assessed 39 patients with metastatic RCC being treated with tyrosine kinase inhibitors and found that entropy decreased and uniformity increased as tumors were treated, suggesting decreasing heterogeneity. Texture uniformity was an independent predictor of time to progression. Kaplan-Meier curves using a uniformity change threshold performed better in stratifying patients without disease progression than standard response assessments including RECIST, Choi criteria, and modified Choi criteria.

Table 3: Pretreatment Assessment with CTTA

Study and Reference	Tumor Type and Number	Imaging Technique	2D versus 3D Imaging	Texture Measure	Statistical Correction	Comments
Lubner et al (37)	157 RCCs (131 ccRCC, 13 pRCC, four chRCC)	Nonenhanced CT, portal venous CECT, heterogeneity in CT vendor and technique	Single section	GLH (TexRAD)	Bonferroni correction	Entropy AUC 0.94 for ccRCC vs other types; entropy, MPP, and SD associated with disease recurrence and death from disease
Schieda et al (39)	RCC (25 ccRCC, 20 sarcomatoid RCC)	Nonenhanced CT, CECT (renal protocol), heterogeneity in CT vendor; CTTA only nonenhanced CT, image intensity normalization	Three axial images	GLCM, RLM (MaZda)	Bonferroni correction	Combined texture features AUC 0.81 for sarcomatoid RCC vs ccRCC; increased run-length nonuniformity and increased gray-level nonuniformity in sarcomatoid RCC
Zhang et al (40)	TCC (106 HG, 18 LG)	Nonenhanced CT, CECT	Single section	GLH (TexRAD)	No	Mean, entropy, MPP, and SD lower in LG tumors; MPP AUC 0.78 for LG vs HG
Sandrasegaran et al (41)	Pancreatic cancer (60 patients)	CECT	Single section	GLH (TexRAD)	Holm correction	Low kurtosis correlated with low OS, high MPP associated with better PFS
Ganeshan et al (45)	Esophageal cancer (21 patients)	Nonenhanced CT	Unclear	GLH (entropy, uniformity)	No	Heterogeneity correlated with SUV_{max}, SUV_{mean}, increased with increasing tumor stage; uniformity independent predictor of survival
Ng et al (6)	CRC (55 patients, primary tumor)	CECT	Primary tumor volume	GLH	No	More homogeneous tumors (lower entropy, higher uniformity, lower SD) had poorer prognosis
Lubner et al (47)	CRC (77 patients, hepatic metastatic disease)	CECT	Single section	GLH (TexRAD)	Bonferroni correction	Entropy, MPP, and SD negatively associated with tumor grade; entropy negatively associated with survival
Ganeshan et al (53)	NSCLC (14 patients)	Nonenhanced CT, CECT	Three sections	GLH	Holm correction	SD and MPP associated with pimonidazole staining (hypoxia); uniformity negatively associated with Glut-1 (hypoxia); MPP negatively associated with CD34 (angiogenesis)
Ganeshan et al (4)	NSCLC (54 patients)	Nonenhanced CT	No data	GLH	No data	PET stage and tumor heterogeneity were independent predictors of survival
Ahn et al (59)	NSCLC (98 unresectable cases treated with CCRT)	CECT	Whole tumor volume	GLH (in-house program)	No	Higher entropy, higher skewness, and higher mean gray-level intensity associated with decreased 3-year OS
Hayano et al (60)	NSCLC (35 patients with metastatic disease treated with antiangiogenic therapy)	Nonenhanced CT for CTTA, CECT (CTP)	Single section	GLH (TexRAD)	No	High MPP and low entropy = favorable PFS and OS; low SUV_{max} = favorable OS; CTP not associated with survival; entropy independent predictor of OS in MV analysis
Zhang et al (8)	SCC of head and neck (72 patients)	CECT, some vendor heterogeneity of CT scanners	Single section	GLH (TexRAD)	No	High entropy and high skewness associated with poor OS; tumor size and nodal stage also associated with OS

Note.—ccRCC = clear cell RCC, CCRT = chemotherapy–radiation therapy, CECT = contrast-enhanced CT, chRCC = chromophobe RCC, CRC = colorectal cancer, CTP = CT perfusion, GLCM = gray-level co-occurrence matrix, GLH = gray-level histogram, HG = high grade, LG = low grade, MV = multivariate, NSCLC = non–small cell lung cancer, OS = overall survival, PFS = progression-free survival, pRCC = papillary RCC, RLM = run-length matrix, SCC = squamous cell carcinoma, SD = standard deviation, TCC = transitional cell carcinoma.

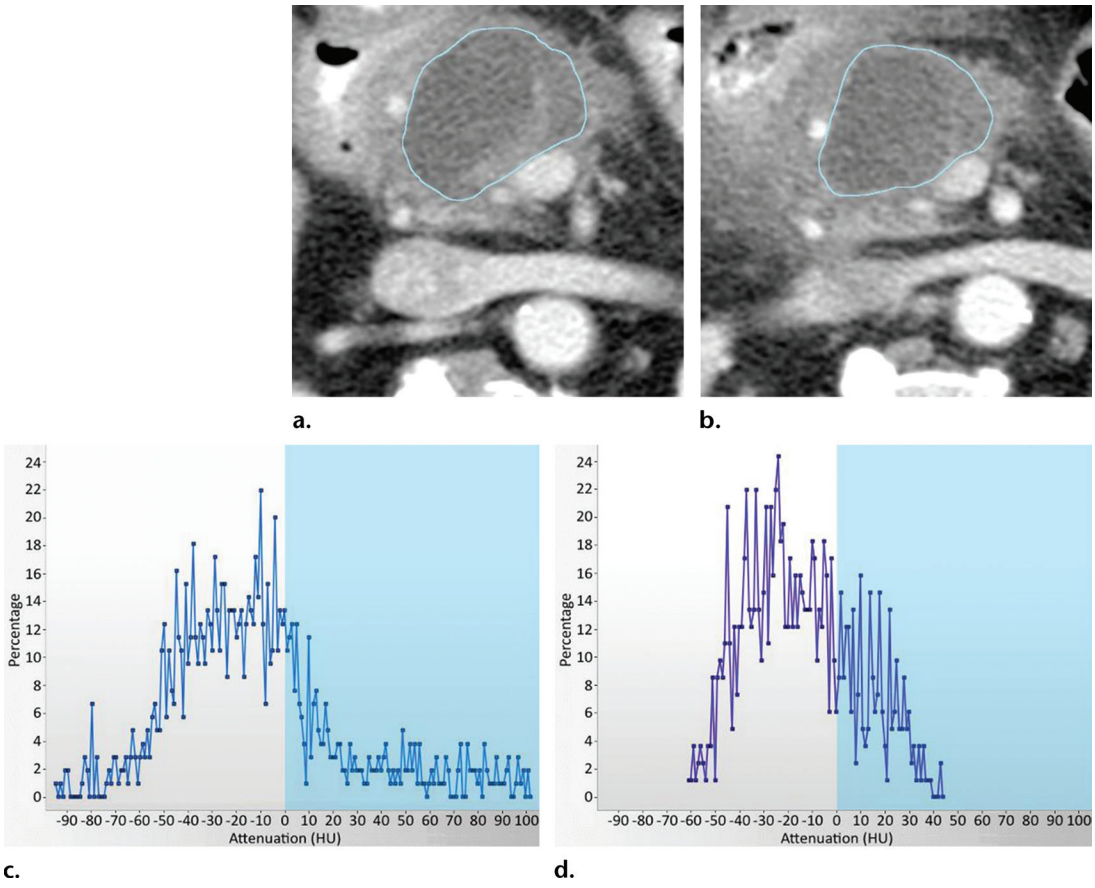

Figure 12. Melanoma. **(a, b)** Baseline CT image **(a)** and initial posttherapy CT image after bevacizumab (antiangiogenic) therapy **(b)** show little change in the lesion. MPP was measured after applying an imaging filter (spatial scaling factor of 4 mm). **(c, d)** CTTA histograms before **(c)** and after **(d)** bevacizumab therapy show a marked reduction in MPP (blue shading), which is associated with increased overall survival.

A group of 20 patients being treated with antiangiogenic therapy and radiation therapy for soft-tissue sarcoma were evaluated with perfusion CT and CT texture features before and after treatment, and changes in blood flow and tumor heterogeneity were calculated. These quantitative imaging findings were correlated with histopathologic results at surgical resection. The percentage change in MPP after 8 weeks of therapy significantly correlated with tumor necrosis in the surgical specimen, while change in tumor size, attenuation alone, and blood flow did not (65).

Similarly, another group evaluated 36 patients with esophageal cancer treated with neoadjuvant chemotherapy and radiation therapy before resection. Tumors with lower posttreatment entropy and higher posttreatment uniformity had improved survival time. Survival models that included texture features in addition to change in esophageal wall thickness performed better than those that included morphologic assessment alone (7,66).

Use of texture to assess response to therapy has also shown some promise in lung, pancreas, and colorectal cancer (35,67–69).

Nononcologic Applications of CTTA

In addition to the oncologic applications, there are a number of emerging nononcologic applications of CTTA, including assessing lung disease such as fibrosis and emphysema (11,70–73), assessing hepatic fibrosis (Fig 13) (13,74) or risk for hepatic failure after resection (9), assessing abdominal aortic aneurysms for risk of rupture (75), and evaluating osseous trabecular texture to detect anorexia nervosa (76). The number of studies is too limited to draw conclusions about the value of CTTA in assessing diffuse disease of the lungs and liver.

Challenges, Limitations, and Unknowns

Although CTTA has shown promise for a wide variety of applications, it still faces challenges to clinical implementation and use (77). As detailed throughout this article, there are multiple platforms for performing CTTA, some commercially available, others custom-made in-house applications. The type of texture analysis performed (statistical-based, model-based, transform-based), the type of segmentation used, postprocessing techniques (filtration, gray-level

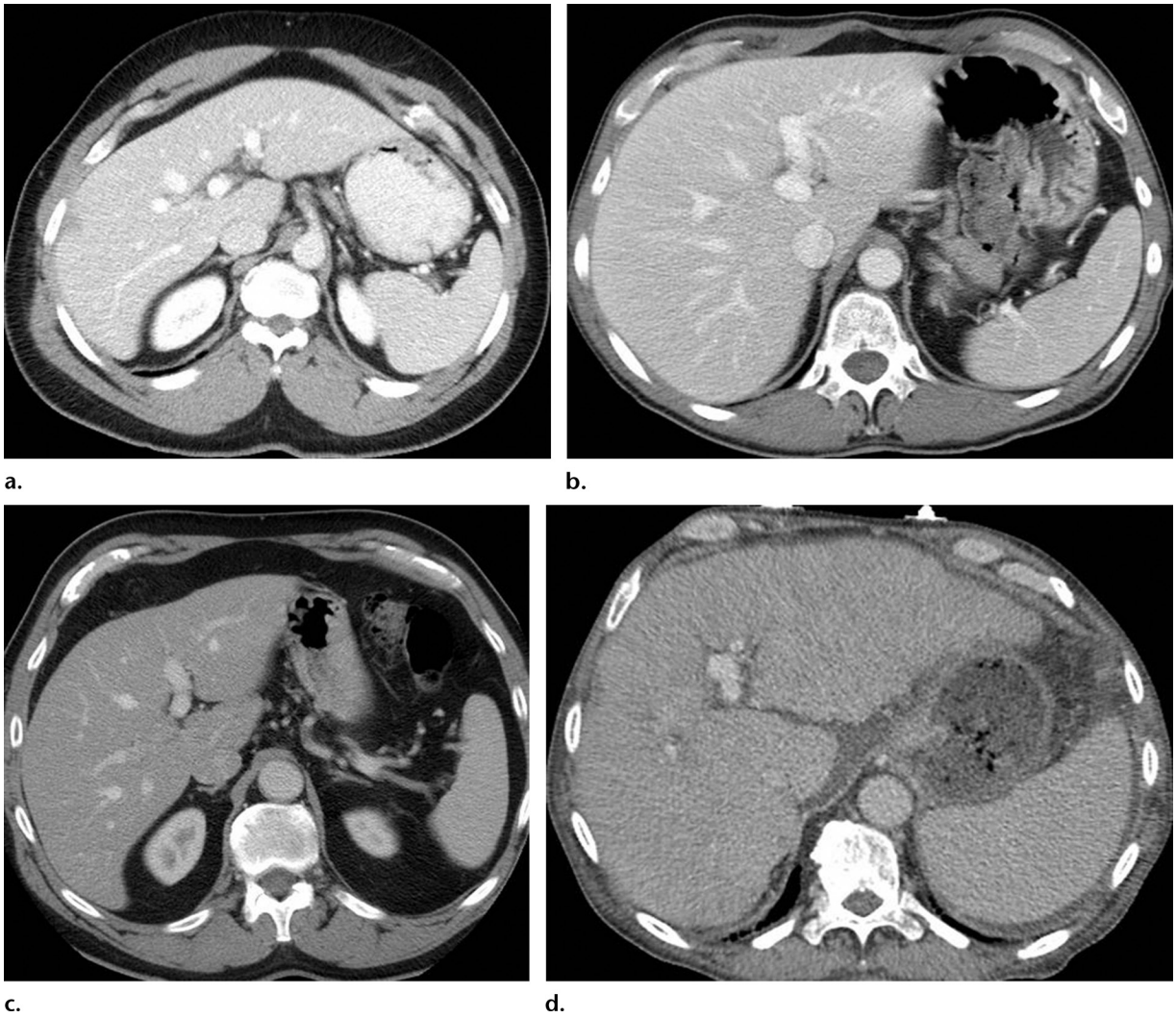

Figure 13. Axial contrast-enhanced CT images of four patients in whom liver biopsy demonstrated varying degrees of hepatic fibrosis. **(a, b)** Stage I **(a)** and stage II **(b)** fibrosis in patients with hepatitis C. **(c)** Stage III fibrosis in a patient with nonalcoholic fatty liver disease. **(d)** Stage IV fibrosis in a patient with liver disease related to both hepatitis C and alcohol use. While these livers become visually a little more heterogeneous, particularly in stage IV, CTTA is able to demonstrate subtle differences in heterogeneity and aid in stratifying the presence and severity of fibrosis (13,74).

normalization), and the quantity and quality of texture feature outputs (first order, higher order) vary widely across different platforms and studies, making comparison between studies and reproduction of study results challenging. Currently, no uniform measurement or reporting standards exist.

Other factors that can introduce variability include lesion morphology and location and imaging acquisition parameters (77–79). For example, the background organ (liver, lung) may affect the lesion texture measurement, and small lesions may have poorer count statistics. In addition, CT acquisition parameters that affect attenuation or pixel relationship clearly have the potential to affect texture measures, although there is some suggestion that first-order texture features may be less affected by changes in technique than mean attenuation (16,78–80).

CTTA is sometimes performed on a single section of the largest cross-sectional diameter of the tumor (2D), while other times it is performed on multiple sections or whole tumor volumes (3D). While it is intuitive that performing a volumetric assessment may provide more data, it is not clear that the extra time and labor associated with volumetric assessment are necessary (15,47). Although reader reproducibility has not been widely assessed, some studies have suggested that single-section measures of first-order statistics are fairly reproducible (19).

When studying multiple lesions, it is not clear what is the best way to combine data. Should texture features of multiple target lesions be summed, averaged, or weighted, or should we look at median values? Similarly, when assessing changes in texture features over time, some studies have evaluated percentage change in

given texture features, while others have used absolute changes or changes beyond a given threshold.

Another major challenge is the sheer amount of data produced by CTTA. The investigation of multiple indexes in a single dataset can lead to significant inflation of type I error and generation of spurious results. A meta-analysis of multiple CT and PET texture analysis studies demonstrated that after applying a statistical correction, many of the 15 included studies no longer demonstrated significant results (81). Use of statistical corrections, such as Holm-Bonferroni sequential correction, or validation datasets may be helpful for confirming the veracity of identified associations (81).

Although multiple studies have described associations between texture features and pathologic or genetic features, establishment of meaningful pathologic correlates is challenging and remains an area of active research. Most, but not all, of the data suggest that more heterogeneous lesions or tumors are more likely to be malignant or biologically aggressive with poorer prognosis, and tumors that become more homogeneous during treatment seem to be responding to therapy. A possible exception to this maxim is colorectal cancer.

In addition, despite the statistically significant results, there is wide variability in the published data and the strength of the described association. For instance, in tumors treated with antiangiogenic therapy, some studies may find entropy to be the best predictor of response, while others find kurtosis to be the best predictor of response. Understanding what these texture features represent on a pathologic, phenotypic, and genetic level may help elucidate why certain tumors have these different radiomic profiles. Nearly all of the publications on CTTA have been from single-center retrospective studies. Going forward, large, multicenter, prospective, hypothesis-driven studies are needed to validate texture analysis as a clinical tool (3).

Future Directions and Clinical Implementation

Although many issues need to be addressed before implementation in clinical practice, an objective tool like CTTA would allow radiologists to obtain additional and more robust CT data from studies that are already being performed. While it is extremely unlikely that CTTA could ever supplant tissue sampling or allow definitive characterization of lesions, certainly if a region of interest can be placed and objective texture features such as entropy evaluated as we would measure Hounsfield units, then the radiologist could get a feel for how heterogeneous a lesion may be. In general, lesions that are more heterogeneous (eg, the more heterogeneous renal lesion seen at nonenhanced CT in Fig 4) may raise the radiologist's concern and trigger additional evaluation, either with additional imaging or with biopsy. While radiologists already do this subjectively, this would provide them with a more objective assessment and may improve their diagnostic confidence.

It would be helpful to have general guidelines about which texture features are most helpful (eg, entropy appears frequently in the literature), general thresholds for what constitutes a heterogeneous lesion, and guidelines for imaging parameters for given texture features and thresholds. It is important to keep in mind that in general, texture data should be obtained from the same organ and during the same phase of contrast enhancement. These types of features could be incorporated into decision-support or computer-aided diagnosis tools.

It is possible that CTTA may be helpful in targeting biopsy, if higher-grade features are seen in more heterogeneous areas of a lesion. CTTA may also have utility in assessing concordance of biopsy results with prior imaging findings. If a lesion appears more heterogeneous or aggressive at imaging but shows a benign biopsy result, it may cue the radiologist to consider repeat biopsy or close imaging follow-up.

Conclusion

CTTA of tumor heterogeneity has shown promise in lesion characterization, pretreatment tumor assessment, and response evaluation for some tumor types. CTTA may also have a spectrum of potential nononcologic applications including assessment of hepatic and pulmonary fibrosis. A variety of challenges, including standardization of segmentation/measurement, postprocessing (eg, use of image filtration methods), and reporting as well as ongoing delineation of pathologic correlates, need to be resolved before widespread implementation.

***Disclosures of Conflicts of Interest.*—M.G.L.** *Activities related to the present article:* disclosed no relevant relationships. *Activities not related to the present article:* grants from Philips and Ethicon. *Other activities:* disclosed no relevant relationships. **A.D.S.** *Activities related to the present article:* disclosed no relevant relationships. *Activities not related to the present article:* president of eMASS LLC, Radiostics LLC, Liver Nodularity LLC, and Color Enhance Detection. *Other activities:* disclosed no relevant relationships. **K.S.** *Activities related to the present article:* disclosed no relevant relationships. *Activities not related to the present article:* consultant for Guerbet Pharmaceuticals. *Other activities:* disclosed no relevant relationships. **P.J.P.** *Activities related to the present article:* disclosed no relevant relationships. *Activities not related to the present article:* cofounder of VirtuoCTC, shareholder in Cellectar Biosciences and SHINE Medical Technologies. *Other activities:* disclosed no relevant relationships.

References

1. Davnall F, Yip CS, Ljungqvist G, et al. Assessment of tumor heterogeneity: an emerging imaging tool for clinical practice? Insights Imaging 2012;3(6):573–589.
2. Haralick RM, Shanmugam K, Dinstein I. Textural features for image classification. IEEE Trans Syst Man Cybern 1973;SMC-3(6):610–621.
3. Bashir U, Siddique MM, Mclean E, Goh V, Cook GJ. Imaging heterogeneity in lung cancer: techniques, applications, and challenges. AJR Am J Roentgenol 2016;207(3):534–543.
4. Ganeshan B, Panayiotou E, Burnand K, Dizdarevic S, Miles K. Tumour heterogeneity in non-small cell lung carcinoma assessed by CT texture analysis: a potential marker of survival. Eur Radiol 2012;22(4):796–802.
5. Miles KA, Ganeshan B, Rodriguez-Justo M, et al. Multifunctional imaging signature for V-KI-RAS2 Kirsten rat sarcoma viral oncogene homolog (KRAS) mutations in colorectal cancer. J Nucl Med 2014;55(3):386–391.
6. Ng F, Ganeshan B, Kozarski R, Miles KA, Goh V. Assessment of primary colorectal cancer heterogeneity by using whole-tumor texture analysis: contrast-enhanced CT texture as a biomarker of 5-year survival. Radiology 2013; 266(1):177–184.
7. Yip C, Landau D, Kozarski R, et al. Primary esophageal cancer: heterogeneity as potential prognostic biomarker in patients treated with definitive chemotherapy and radiation therapy. Radiology 2014;270(1):141–148.
8. Zhang H, Graham CM, Elci O, et al. Locally advanced squamous cell carcinoma of the head and neck: CT texture and histogram analysis allow independent prediction of overall survival in patients treated with induction chemotherapy. Radiology 2013;269(3):801–809.
9. Simpson AL, Adams LB, Allen PJ, et al. Texture analysis of preoperative CT images for prediction of postoperative hepatic insufficiency: a preliminary study. J Am Coll Surg 2015;220(3):339–346.
10. Park SO, Seo JB, Kim N, Lee YK, Lee J, Kim DS. Comparison of usual interstitial pneumonia and nonspecific interstitial pneumonia: quantification of disease severity and discrimination between two diseases on HRCT using a texture-based automated system. Korean J Radiol 2011;12(3):297–307.
11. Park HJ, Lee SM, Song JW, et al. Texture-based automated quantitative assessment of regional patterns on initial CT in patients with idiopathic pulmonary fibrosis: relationship to decline in forced vital capacity. AJR Am J Roentgenol 2016;207(5):976–983.
12. Park YS, Seo JB, Kim N, et al. Texture-based quantification of pulmonary emphysema on high-resolution computed tomography: comparison with density-based quantification and correlation with pulmonary function test. Invest Radiol 2008;43(6):395–402.
13. Daginawala N, Li B, Buch K, et al. Using texture analyses of contrast enhanced CT to assess hepatic fibrosis. Eur J Radiol 2016;85(3):511–517.
14. Ganeshan B, Miles KA. Quantifying tumour heterogeneity with CT. Cancer Imaging 2013;13:140–149.
15. Ng F, Kozarski R, Ganeshan B, Goh V. Assessment of tumor heterogeneity by CT texture analysis: can the largest cross-sectional area be used as an alternative to whole tumor analysis? Eur J Radiol 2013;82(2):342–348.
16. Ganeshan B, Burnand K, Young R, Chatwin C, Miles K. Dynamic contrast-enhanced texture analysis of the liver: initial assessment in colorectal cancer. Invest Radiol 2011;46(3):160–168.
17. Ganeshan B, Miles KA, Young RC, Chatwin CR. In search of biologic correlates for liver texture on portal-phase CT. Acad Radiol 2007;14(9):1058–1068.
18. Ganeshan B, Miles KA, Young RC, Chatwin CR. Texture analysis in non-contrast enhanced CT: impact of malignancy on texture in apparently disease-free areas of the liver. Eur J Radiol 2009;70(1):101–110.
19. Smith AD, Gray MR, del Campo SM, et al. Predicting overall survival in patients with metastatic melanoma on antiangiogenic therapy and RECIST stable disease on initial posttherapy images using CT texture analysis. AJR Am J Roentgenol 2015;205(3):W283–W293.
20. Raman SP, Chen Y, Schroeder JL, Huang P, Fishman EK. CT texture analysis of renal masses: pilot study using random forest classification for prediction of pathology. Acad Radiol 2014;21(12):1587–1596.
21. Yan L, Liu Z, Wang G, et al. Angiomyolipoma with minimal fat: differentiation from clear cell renal cell carcinoma and papillary renal cell carcinoma by texture analysis on CT images. Acad Radiol 2015;22(9):1115–1121.
22. Hodgdon T, McInnes MD, Schieda N, Flood TA, Lamb L, Thornhill RE. Can quantitative CT texture analysis be used to differentiate fat-poor renal angiomyolipoma from renal cell carcinoma on unenhanced CT images? Radiology 2015;276(3):787–796.
23. Takahashi N, Takeuchi M, Sasaguri K, Leng S, Froemming A, Kawashima A. CT negative attenuation pixel distribution and texture analysis for detection of fat in small angiomyolipoma on unenhanced CT. Abdom Radiol (NY) 2016;41(6):1142–1151.
24. Leng S, Takahashi N, Gomez Cardona D, et al. Subjective and objective heterogeneity scores for differentiating small renal masses using contrast-enhanced CT. Abdom Radiol (NY) 2017;42(5):1485–1492.
25. Canellas R, Mehrkhani F, Patino M, Kambadakone A, Sahani D. Characterization of portal vein thrombosis (neoplastic versus bland) on CT images using software-based texture analysis and thrombus density (Hounsfield units). AJR Am J Roentgenol 2016;207(5):W81–W87.
26. Raman SP, Schroeder JL, Huang P, et al. Preliminary data using computed tomography texture analysis for the classification of hypervascular liver lesions: generation of a predictive model on the basis of quantitative spatial frequency measurements—a work in progress. J Comput Assist Tomogr 2015;39(3):383–395.
27. Hanania AN, Bantis LE, Feng Z, et al. Quantitative imaging to evaluate malignant potential of IPMNs. Oncotarget 2016;7(52):85776–85784.
28. Hu Y, Liang Z, Song B, et al. Texture feature extraction and analysis for polyp differentiation via computed tomography colonography. IEEE Trans Med Imaging 2016;35(6):1522–1531.
29. Song B, Zhang G, Lu H, et al. Volumetric texture features from higher-order images for diagnosis of colon lesions via CT colonography. Int J CARS 2014;9(6):1021–1031.
30. Pooler BD, Lubner MG, Hu Y, et al. Volumetric textural analysis of colorectal masses at CT colonography: differentiating benign from malignant pathology and comparison with human readers [abstr]. In: Radiological Society of North America Scientific Assembly and Annual Meeting Program. Oak Brook, Ill: Radiological Society of North America, 2016; 152.
31. Dennie C, Thornhill R, Sethi-Virmani V, et al. Role of quantitative computed tomography texture analysis in the differentiation of primary lung cancer and granulomatous nodules. Quant Imaging Med Surg 2016;6(1):6–15.
32. Lee SH, Lee SM, Goo JM, Kim KG, Kim YJ, Park CM. Usefulness of texture analysis in differentiating transient from persistent part-solid nodules (PSNs): a retrospective study. PLoS One 2014;9(1):e85167.
33. Suo S, Cheng J, Cao M, et al. Assessment of heterogeneity difference between edge and core by using texture analysis: differentiation of malignant from inflammatory pulmonary nodules and masses. Acad Radiol 2016;23(9):1115–1122.
34. Andersen MB, Harders SW, Ganeshan B, Thygesen J, Torp Madsen HH, Rasmussen F. CT texture analysis can help differentiate between malignant and benign lymph nodes in the mediastinum in patients suspected for lung cancer. Acta Radiol 2016;57(6):669–676.
35. Mattonen SA, Palma DA, Haasbeek CJ, Senan S, Ward AD. Early prediction of tumor recurrence based on CT texture changes after stereotactic ablative radiotherapy (SABR) for lung cancer. Med Phys 2014;41(3):033502.
36. Mattonen SA, Tetar S, Palma DA, Louie AV, Senan S, Ward AD. Imaging texture analysis for automated prediction of lung cancer recurrence after stereotactic radiotherapy. J Med Imaging (Bellingham) 2015;2(4):041010.
37. Lubner MG, Stabo N, Abel EJ, Del Rio AM, Pickhardt PJ. CT textural analysis of large primary renal cell carcinomas:

pretreatment tumor heterogeneity correlates with histologic findings and clinical outcomes. AJR Am J Roentgenol 2016;207(1):96–105.
38. Scrima AN, Lubner MG, Abel EJ, Pickhardt PJ. CT textural analysis of small renal masses. Madison, Wis: University of Wisconsin School of Medicine and Public Health, 2016.
39. Schieda N, Thornhill RE, Al-Subhi M, et al. Diagnosis of sarcomatoid renal cell carcinoma with CT: evaluation by qualitative imaging features and texture analysis. AJR Am J Roentgenol 2015;204(5):1013–1023.
40. Zhang GM, Sun H, Shi B, Jin ZY, Xue HD. Quantitative CT texture analysis for evaluating histologic grade of urothelial carcinoma. Abdom Radiol (NY) 2017;42(2):561–568.
41. Sandrasegaran K, Lin C, Asare-Sawiri M, Lin Y. CT texture analysis of pancreatic cancer. Presented at the Annual Scientific Meeting and Educational Course of the Society of Abdominal Radiology, Waikoloa, Hawaii, March 13–18, 2016.
42. Canellas R, Bhowmik S, Almeida RR, Burk KS, McDermott S, Sahani DV. Prediction of pancreatic neuroendocrine tumor grade on CT images using a software based texture analysis [abstr]. In: Radiological Society of North America Scientific Assembly and Annual Meeting Program. Oak Brook, Ill: Radiological Society of North America, 2016; 143.
43. Li M, Fu S, Zhu Y, et al. Computed tomography texture analysis to facilitate therapeutic decision making in hepatocellular carcinoma. Oncotarget 2016;7(11):13248–13259.
44. Fu S, Chen S, Liang C, et al. Texture analysis of intermediate-advanced hepatocellular carcinoma: prognosis and patients' selection of transcatheter arterial chemoembolization and sorafenib. Oncotarget 2017;8(23):37855–37865.
45. Ganeshan B, Skogen K, Pressney I, Coutroubis D, Miles K. Tumour heterogeneity in oesophageal cancer assessed by CT texture analysis: preliminary evidence of an association with tumour metabolism, stage, and survival. Clin Radiol 2012;67(2):157–164.
46. Yoon SH, Kim YH, Lee YJ, et al. Tumor heterogeneity in human epidermal growth factor receptor 2 (HER2)-positive advanced gastric cancer assessed by CT texture analysis: association with survival after trastuzumab treatment. PLoS One 2016;11(8):e0161278.
47. Lubner MG, Stabo N, Lubner SJ, et al. CT textural analysis of hepatic metastatic colorectal cancer: pre-treatment tumor heterogeneity correlates with pathology and clinical outcomes. Abdom Imaging 2015;40(7):2331–2337.
48. André T, Boni C, Navarro M, et al. Improved overall survival with oxaliplatin, fluorouracil, and leucovorin as adjuvant treatment in stage II or III colon cancer in the MOSAIC trial. J Clin Oncol 2009;27(19):3109–3116.
49. Ganeshan B, Miles KA, Young RC, Chatwin CR. Hepatic enhancement in colorectal cancer: texture analysis correlates with hepatic hemodynamics and patient survival. Acad Radiol 2007;14(12):1520–1530.
50. Miles KA, Ganeshan B, Griffiths MR, Young RC, Chatwin CR. Colorectal cancer: texture analysis of portal phase hepatic CT images as a potential marker of survival. Radiology 2009;250(2):444–452.
51. Rao SX, Lambregts DM, Schnerr RS, et al. Whole-liver CT texture analysis in colorectal cancer: does the presence of liver metastases affect the texture of the remaining liver? United European Gastroenterol J 2014;2(6):530–538.
52. Lee SJ, Lubner MG, Kim DK, Pickhardt PJ. Can texture features predict imminent development of hepatic colorectal metastatic disease? Presented at the Annual Meeting of the European Society of Gastrointestinal and Abdominal Radiology, Athens, Greece, June 20–23, 2017.
53. Ganeshan B, Goh V, Mandeville HC, Ng QS, Hoskin PJ, Miles KA. Non–small cell lung cancer: histopathologic correlates for texture parameters at CT. Radiology 2013;266(1):326–336.
54. Weiss GJ, Ganeshan B, Miles KA, et al. Noninvasive image texture analysis differentiates K-ras mutation from pan-wildtype NSCLC and is prognostic. PLoS One 2014;9(7):e100244.
55. Ozkan E, West A, Dedelow JA, et al. CT gray-level texture analysis as a quantitative imaging biomarker of epidermal growth factor receptor mutation status in adenocarcinoma of the lung. AJR Am J Roentgenol 2015;205(5):1016–1025.
56. Liu Y, Kim J, Balagurunathan Y, et al. Radiomic features are associated with EGFR mutation status in lung adenocarcinomas. Clin Lung Cancer 2016;17(5):441–448.e6.
57. Gevaert O, Xu J, Hoang CD, et al. Non–small cell lung cancer: identifying prognostic imaging biomarkers by leveraging public gene expression microarray data—methods and preliminary results. Radiology 2012;264(2):387–396.
58. Ganeshan B, Abaleke S, Young RC, Chatwin CR, Miles KA. Texture analysis of non-small cell lung cancer on unenhanced computed tomography: initial evidence for a relationship with tumour glucose metabolism and stage. Cancer Imaging 2010;10:137–143.
59. Ahn SY, Park CM, Park SJ, et al. Prognostic value of computed tomography texture features in non-small cell lung cancers treated with definitive concomitant chemoradiotherapy. Invest Radiol 2015;50(10):719–725.
60. Hayano K, Kulkarni NM, Duda DG, Heist RS, Sahani DV. Exploration of imaging biomarkers for predicting survival of patients with advanced non-small cell lung cancer treated with antiangiogenic chemotherapy. AJR Am J Roentgenol 2016;206(5):987–993.
61. Miles KA. How to use CT texture analysis for prognostication of non-small cell lung cancer. Cancer Imaging 2016;16:10.
62. Ganeshan B, Miles KA, Babikir S, et al. CT-based texture analysis potentially provides prognostic information complementary to interim FDG-PET for patients with Hodgkin's and aggressive non-Hodgkin's lymphomas. Eur Radiol 2017;27(3):1012–1020.
63. Fujita A, Buch K, Li B, Kawashima Y, Qureshi MM, Sakai O. Difference between HPV-positive and HPV-negative non-oropharyngeal head and neck cancer: texture analysis features on CT. J Comput Assist Tomogr 2016;40(1):43–47.
64. Goh V, Ganeshan B, Nathan P, Juttla JK, Vinayan A, Miles KA. Assessment of response to tyrosine kinase inhibitors in metastatic renal cell cancer: CT texture as a predictive biomarker. Radiology 2011;261(1):165–171.
65. Tian F, Hayano K, Kambadakone AR, Sahani DV. Response assessment to neoadjuvant therapy in soft tissue sarcomas: using CT texture analysis in comparison to tumor size, density, and perfusion. Abdom Imaging 2015;40(6):1705–1712.
66. Yip C, Davnall F, Kozarski R, et al. Assessment of changes in tumor heterogeneity following neoadjuvant chemotherapy in primary esophageal cancer. Dis Esophagus 2015;28(2):172–179.
67. Chong Y, Kim JH, Lee HY, et al. Quantitative CT variables enabling response prediction in neoadjuvant therapy with EGFR-TKIs: are they different from those in neoadjuvant concurrent chemoradiotherapy? PLoS One 2014;9(2):e88598.
68. Rao SX, Lambregts DM, Schnerr RS, et al. CT texture analysis in colorectal liver metastases: a better way than size and volume measurements to assess response to chemotherapy? United European Gastroenterol J 2016;4(2):257–263.
69. Ahn SJ, Kim JH, Park SJ, Han JK. Prediction of the therapeutic response after FOLFOX and FOLFIRI treatment for patients with liver metastasis from colorectal cancer using computerized CT texture analysis. Eur J Radiol 2016;85(10):1867–1874.
70. Chong DY, Kim HJ, Lo P, et al. Robustness-driven feature selection in classification of fibrotic interstitial lung disease patterns in computed tomography using 3D texture features. IEEE Trans Med Imaging 2016;35(1):144–157.
71. Korfiatis PD, Karahaliou AN, Kazantzi AD, Kalogeropoulou C, Costaridou LI. Texture-based identification and characterization of interstitial pneumonia patterns in lung multidetector CT. IEEE Trans Inf Technol Biomed 2010;14(3):675–680.
72. Alemzadeh M, Boylan C, Kamath MV. Review of texture quantification of CT images for classification of lung diseases. Crit Rev Biomed Eng 2015;43(2-3):183–200.
73. Ginsburg SB, Zhao J, Humphries S, et al. Texture-based quantification of centrilobular emphysema and centrilobular nodularity in longitudinal CT scans of current and former smokers. Acad Radiol 2016;23(11):1349–1358.
74. Lubner MG, Malecki K, Kloke J, Ganeshan B, Pickhardt PJ. Texture analysis of the liver at MDCT for assessing hepatic fibrosis. Abdom Radiol (NY) 2017 Mar 17. [Epub ahead of print]

75. Kotze CW, Rudd JH, Ganeshan B, et al. CT signal heterogeneity of abdominal aortic aneurysm as a possible predictive biomarker for expansion. Atherosclerosis 2014;233(2):510–517.
76. Tabari A, Torriani M, Miller KK, Klibanski A, Kalra MK, Bredella MA. Anorexia nervosa: analysis of trabecular texture with CT. Radiology 2017;283(1):178–185.
77. Summers RM. Texture analysis in radiology: does the emperor have no clothes? Abdom Radiol (NY) 2017;42(2):342–345.
78. Shafiq-Ul-Hassan M, Zhang GG, Latifi K, et al. Intrinsic dependencies of CT radiomic features on voxel size and number of gray levels. Med Phys 2017;44(3):1050–1062.
79. Lu L, Ehmke RC, Schwartz LH, Zhao B. Assessing agreement between radiomic features computed for multiple CT imaging settings. PLoS One 2016;11(12):e0166550.
80. Mackin D, Fave X, Zhang L, et al. Measuring computed tomography scanner variability of radiomics features. Invest Radiol 2015;50(11):757–765.
81. Chalkidou A, O'Doherty MJ, Marsden PK. False discovery rates in PET and CT studies with texture features: a systematic review. PLoS One 2015;10(5):e0124165.

This journal-based SA-CME activity has been approved for ***AMA PRA Category 1 Credit™.*** *See www.rsna.org/education/search/RG.*